

Human-inspired Motion Planning for Omni-directional Social Robots

Ryo Kitagawa
Kyoto University
Kyoto, Japan

Yuyi Liu
Kyoto University
Kyoto, Japan
ATR
Kyoto, Japan
yuyi.liu@robot.soc.i.kyoto-u.ac.jp

Takayuki Kanda
Kyoto University
Kyoto, Japan
ATR
Kyoto, Japan

ABSTRACT

Omni-directional robots have gradually been popular for social interactions with people in human environments. The characteristics of omni-directional bases allow the robots to change their body orientation freely while moving straight. However, human spectators show dislike when observing robots behave unnaturally. In this paper, we observed how humans naturally move to goals and then developed a motion planning algorithm for omni-directional robots to resemble human movements in a time-efficient manner. Instead of treating the translation and rotation of a robot separately, the proposed motion planner couples the two motions with constraints inspired from the observation of human behaviors. We implemented the proposed method onto an omni-directional robot and conducted navigation experiments in a shop with shelves and narrow corridors at width of 90cm. Results from a within-participants study of 300 human spectators validated that the proposed human-inspired motion planner provided people with more natural and predictable feelings compared to the common rotate-while-move or rotate-then-move strategies.

CCS CONCEPTS

- Human-centered computing → Social navigation; User studies;
- Computer systems organization → Robotic control.

KEYWORDS

Omni-directional Robot, Social Navigation, Motion Planning, Social Robot

ACM Reference Format:

Ryo Kitagawa, Yuyi Liu, and Takayuki Kanda. 2021. Human-inspired Motion Planning for Omni-directional Social Robots. In *Proceedings of the 2021 ACM/IEEE International Conference on Human-Robot Interaction (HRI '21), March 8–11, 2021, Boulder, CO, USA*. ACM, New York, NY, USA, 9 pages. <https://doi.org/10.1145/3434073.3444679>

1 INTRODUCTION

Mobile robots have started to navigate and interact with people in public spaces, such as hotels, shopping malls [14], and museums

Permission to make digital or hard copies of all or part of this work for personal or classroom use is granted without fee provided that copies are not made or distributed for profit or commercial advantage and that copies bear this notice and the full citation on the first page. Copyrights for components of this work owned by others than ACM must be honored. Abstracting with credit is permitted. To copy otherwise, or republish, to post on servers or to redistribute to lists, requires prior specific permission and/or a fee. Request permissions from permissions@acm.org.

HRI '21, March 8–11, 2021, Boulder, CO, USA
© 2021 Association for Computing Machinery.
ACM ISBN 978-1-4503-8289-2/21/03...\$15.00
<https://doi.org/10.1145/3434073.3444679>

[2]. Omni-directional wheeled base is recently becoming a popular platform for the robots moving in human environments (such as Pepper [15]). Different from the classic design of a differential-drive base (like Pioneer 3-DX, etc.) that is most commonly deployed for mobile robots with social applications, omni-directional bases allow robots, as we humans, to change their body orientation while moving straight.

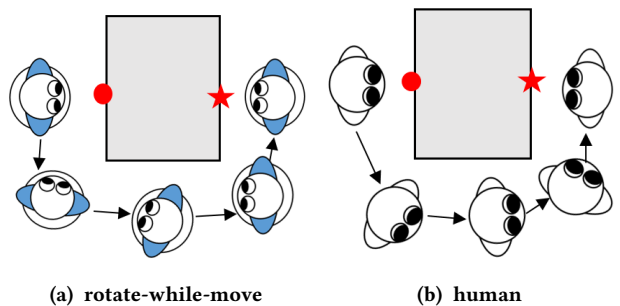


Figure 1: Typical paths of a omni-directional robot (a) and a person (b) while changing the pose from one side (red circle mark) to the opposite side (red star mark).

However, people show their dislike to the behaviors of omni-based robots when watching robot moving. The feeling of discomfort falls on multiple perspectives, such as low anthropomorphism and low predictability. Namely, the movements of omni-directional robots does not resemble the behaviors of a normal human. An intuitive example is illustrated in Fig.1. In a daily situation that a person changes his or her standing position from one-side of a table (a red circle mark) to another side (a red star mark), a typical person moves in a trajectory as shown in Fig.1b. While a typical omni-directional robot (see Fig.1a) would simultaneously rotate and move aside first, say "*rotate-while-move*", then keep backward movement and finally slide to the goal without extra rotation.

Why does such big difference in movement between a robot and a typical person occur? Unlike the human locomotion with constraints on limbs, an omni-directional base is with a fully decoupled kinematics between translation and rotation motions. This characteristics of omni-based robots further leads to a typical "*functional*" planning strategy to optimally control robots' translation and rotation in a separate fashion.

Assuming that to have a robot behave in a more human-like style is an explicit way to increase trust and preference by human beings, we are interested in understanding how to resemble human movements for the omni-directional robots. Hence, in this paper,

we arise the following questions that have been seldom explored and propose answers to them, namely:

- Why do people move in the way we currently behave from the aspect of kinematics?
- How can an omni-directional robot behave more human-like as we naturally move, despite of its big difference in kinematics with human locomotion?

2 RELATED WORK

2.1 Social-Aware Navigation

Classical navigation approaches treat people in public areas as dynamic obstacles for robots [11, 23], which usually generate confusing movements in front of people [18]. In recent decade, researchers have started to develop methods that are more socially acceptable by human [19, 24]. Some research focuses on modelling the paths of the pedestrians nearby the robot. In [26], a pedestrian model was built to predict the paths of approaching people for the robot to avoid them in a social distance. Non-cooperative game theory was applied to demonstrate the decision making of human in crossing interaction in [27]. Authors in [17] proposed an adaptive motion model for the indents of pedestrians based on velocity-space reasoning concept. While some previous works modelled the impact of pedestrians in the environment by accounting for social interactions as parameters, e.g. extended social force models [10, 28].

In comparison, there has also been research conducted to resemble human behaviors by using learning-based methods. Luber et al. [21] proposed a unsupervised learning method that meets the criteria such as social comfort together with path-efficiency for social navigation among people. A probability distribution over the cluster of trajectories with pedestrians nearby was applied into a reward function in learning framework for social-compliant robot navigation [18]. Chen et al. [5] deployed a time-efficient navigation method that used deep reinforcement learning to respects common social forms for a robotic vehicle in a pedestrian-rich area. Inverse reinforcement learning was utilized to predict human's decision in an orthogonal crossing interaction in [4].

Whether using model-based or learning-based methods, previous research simplifies human behaviors as motions of a particle. Body orientation of human is not taken into account. With the consideration of robot orientation in navigation, robots will have better predictability by moving in more human-like manners, thus obtain socially acceptance from not only those who directly interact with robots, but also the observers who watch the robot motions.

2.2 Predictability by Human Observers

Researchers have started to explore the efficiency of human-robot interaction and collaboration [8, 12] since last decades. Dragan et al. [9] proposed that predictability to describe how human observers can expect robot motions with no surprise, is one of the criteria that affects human-robot collaboration. The authors further demonstrated the effects of "predictable" robot motions via human-robot collaboration experiments in [8]. They found that pure "functional" (e.g. distance-efficient collision-free trajectory to a target) robot motions did harm to collaboration.

In [29], the authors used a labeling scheme to measure the predictability of robot task planning. They further proposed strategy to synthesize plans that were more easily understood by humans.

The researchers [6] implemented theory of mind to make robot predictable to people to improve human-robot collaboration. Namely, the robot provided the human partner information about what he missed during the temporary absence.

By far, previous works are all keen on the applications of robotic arms in human-robot collaboration. Seldom research about this topic has been explored on mobile robots.

2.3 Omni-Directional Robots

Omni-directional robots, such as commercially-available Turtlebot and Pepper, have been broadly deployed in human environments since last two decades. Research about omni-directional robots has been carried out on motion control [20] and special design [3], etc.

Seldom navigation methods have been specially designed for omni-directional robots. Only by recent have works started to utilize the "extra DOF" of omni-directional robots to generate more social-compliant paths. The authors in [22] proposed a path planner inspired from human guard motions in the shopping mall. The specific planner required a robot for simultaneous sliding and rotation movements, which does not fit differential-drive locomotion. In [25], a "body rotation and sliding" manner was deployed to a path planner for an omni-directional robot to behave politely in crossing interaction in narrow environments e.g. a corridor in a store.

Previous works mainly focused on how an omni-directional robot can handle specific situations, e.g. crossing, passing or approaching interaction, in a social-compliant way. However, it is still unclear whether there is a unified motion planning strategy for omni-directional robots to navigate in a more human-like manner.

3 MODELLING NATURAL MOVEMENT OF HUMANS

We start from investigating how we humans naturally move. The observations mainly focus on the kinematics of rotation and translation in human movements.

3.1 Observation of How Human Moves

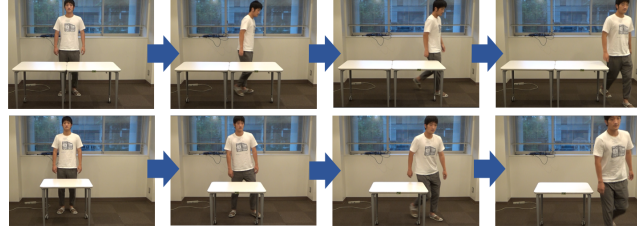
We first carried out observations in a lab. A group of people were asked to move in daily scenarios (from here to there). We observed their behaviors one after another. We illustrate some representative case in Fig.2 to explain findings from the observations. In Fig.2a, a person was asked to reach for a goal behind him in an empty room twice. In the second trial, we changed the goal relatively far from him. He moved in two different ways. To reach for a nearby goal, he only moved backward. While he generated a trajectory to the farther goal with rotation, forward movement and extra rotation.

It is interesting that people behave differently in similar environments. To reach for the goal close behind, at least in our first inspiration, one-step backward movement seems more time-saving, i.e. optimal. In contrast, if a goal is far behind, the choice to turn around, move forward and finally turn back seems more reasonable, since it is more time-efficient than keeping backward movements.

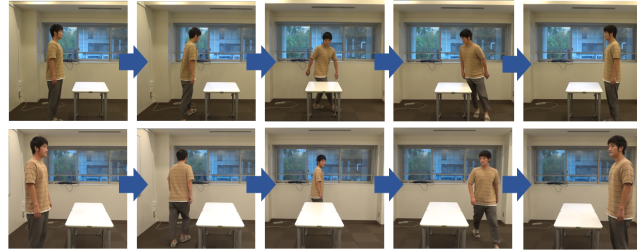
In Fig.2b, the person moved in two different ways to pass around the table and move to the goal. To bypass a long table, the person



(a) People move backward to a nearby goal behind. However when the goal is far, people turn around and move.



(b) People rotate and move when an obstacle is large, while they slide to avoid small obstacles.



(c) Two different plans to reach for the opposite side of a table.

Figure 2: Examples of human's movements

chose to rotate and move forward. While to avoid a smaller table, he chose to laterally slid and further moved forward. Compared with other ways to move in the same environment, the movements people chose are the more time-saving. In Fig.2c, the person chose to pass around a small table via sliding and rotation. While the person chose to rotate and keep moving forward in the case that he needed to move a long distance. Still in this case, people chose more time-saving ways to move according to the specific environment.

Such kind of plain optimization, i.e. taking the most time-saving way to move, reflects why people choose different motions case by case. Largely, people's motion is optimal, as the observed motion is the more efficient combination among other possible movements. Provided that humans have been kept the current locomotion over hundred thousand years, we optimize how we move subconsciously, or say, naturally.

Apart from rotation, we broadly classify the specific human movement into three categories, i.e. forward, sliding, backward. For a person, each specific movement is with different top speed, thus provides different time-efficiency. People prefer most to move forward, since it is the fastest way to move. Sliding movement would take more time compared with forward movement. Still, it is faster than backward movement. Also, people rarely move backward because this movement is the slowest.

3.2 Speculation on Human Movement

How to reproduce human motions in omni-directional robots? There exists speed difference among specific human movements. Considering that we prefer to move in a more time-saving way, keeping forward movement is the best choice when possible. However in daily scenarios, the environment is always complicated. This requires people to combine different kinds of movement together.

In Fig.2b, the person needed to first bypass the long table, then reach for the goal at right bottom. Thus his motion can be treated in two parts, i.e. locally to bypass the table and globally to arrive at goal. As illustrated in Fig.3, there are three potential combinations of movements to reach for the goal. If we assume that people optimize the motions locally, then in the first part of motion, people should only take bypassing table into account. Consequently, (b) and (c) would be both optimal choices. However, in fact only the diagonal trajectory in (b) represents a typical choice by people, which is inconsistent with our assumption.

In contrast, the assumption that people optimize their motion from a global aspect reflects why people are more goal-conscious after passing around the table. Simply, when we comparing the second half path in (b) and (c), (b) is obviously more time-saving. In short, global optimum is chosen.

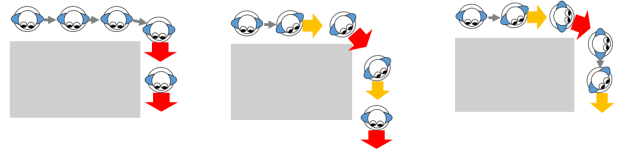


Figure 3: Speculation on how to reproduce human motions.

3.3 Modelling of Human Kinematic Constraint

As described in previous section, people optimize their motion by maximizing fastest forward movement and minimizing slower lateral sliding or backward movements. What leads to the speed difference among these specific movements?

We generally answer this question based on the observation of simple human movements. Namely,

- 1) people have to slow down when their moving direction differs from their body orientation.
- 2) people have to slow down when rotating.

Fig.4 illustrates the above two kinematic constraints in human movement. The first constraint on moving direction generally represents why people prefer to move forward most, rather than to move aside or backward all the time. Meanwhile, the second constraint on rotation explains why people move sideways or backward to reach for a goal nearby, instead of rotating and then moving forward.

We model these two kinematic constraints to explain various human movement behaviors in a unified way. In particular, rather than precisely modelling human movement kinematics, we design the constraints in the form of trigonometric function, since they generally suffice to the characteristics of human movements, e.g. forward movement is fastest while backward movement is slowest.

Based on the observation of people slowing down when moving with large heading angles, The constraint on translation is described

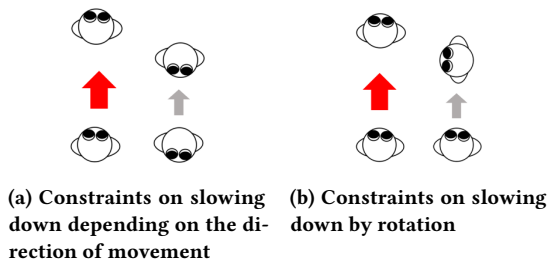
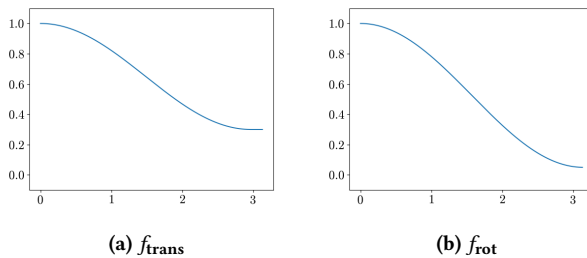


Figure 4: Illustrations of kinematic constraints

Figure 5: constraints curve. (a) shows when $\alpha = 0.3$ and $\beta = \frac{17\pi}{18}$. (b) shows when $\gamma = 0.05$.

as Eq.(1) (See Fig.5a), which represents the speed rate at certain situation relative to people's max speed. θ denotes the heading angle between current body orientation and the direction of travel. α and β represents parameters. Later, in Sec.5, these parameters will be calibrated using human trajectory data.

When the direction of travel coincides the current body orientation, $\theta = 0$, thus $f_{trans} = 1$, meaning that people move at full speed. When people move backward, $\theta = \pi$, thus $f_{trans} = \alpha$. For instance, if $\alpha = 0.3$, people would be modeled to move backward only at 30% of their max speed.

$$f_{trans}(\theta) = \begin{cases} \frac{1-\alpha}{2} \cos \frac{\theta}{\beta} + \frac{1+\alpha}{2} & 0 \leq \theta \leq \beta \\ \alpha & \beta < \theta \leq \pi \end{cases} \quad (1)$$

Similarly, considering that people cannot translate fast when rotating fast, we set the constraint on rotation in Eq.(2). The function displays the speed rate relative to people's max speed when rotating. ω represents the human rotational speed and is within the range of $0 \leq \omega \leq \omega_{max}$. γ denotes the constant parameter to be identified in Sec.5. When there is no body rotation, $\omega = 0$, then $f_{rot} = 1$, as is shown in Fig.5b. While when people rotate rather fast, say $\omega = \omega_{max}$, $f_{rot} = \gamma$.

$$f_{rot}(\omega) = \begin{cases} \frac{1-\gamma}{2} \cdot \cos \omega + \frac{1+\gamma}{2} & 0 \leq \omega \leq \pi \\ \gamma & \pi < \omega \leq \omega_{max} \end{cases} \quad (2)$$

4 IMPLEMENTATION

The proposed human-inspired time-efficient path planning algorithm is implemented on an omni-directional robot.

4.1 Architecture

The whole framework of navigation system is shown in Fig.6. The localization module (Sec.4.5) estimates the robot pose based on the

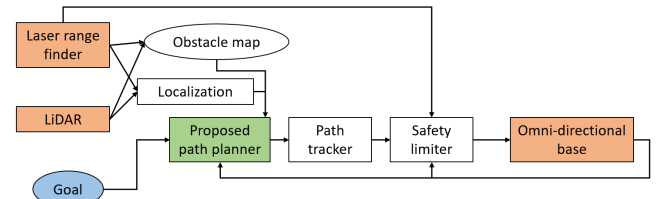


Figure 6: Diagram of implementation of proposed navigation framework on the robot.

sensor data from the LiDAR and laser scanners; An obstacle map was built based on the collected pointcloud data. The real-time robot pose and obstacle map are passed to the proposed path planner (Sec.4.3), where a collision-free path that resembles human movements, including straight forward moving, rotating, and sliding motions, is generated to a prescribed goal pose. The path tracker (Sec.4.4) then outputs desired velocity commands for robot to follow the path. The safety limiter (Sec.4.6) feeds the safe velocity commands to the omni-directional base at 10Hz.

4.2 Robot Hardware

A Robovie R3 with a human-like appearance and a height of 120cm is deployed, as shown in Fig.10. The robot with an omni-directional base can move in any direction at a maximum speed of 1.5 m/s and a maximum angular velocity of 2 rad/s. The robot is outfitted with a Velodyne HDL-32E LiDAR at the back top of its upper body and four Hokuyo UTM-30LX laser range finders on its bottom base.

4.3 Human-Movement-Inspired Path Planner

As discussed in Sec.3, we anticipate that humans optimize motion in a global manner with certain kinds of kinematic constraints due to physical restrictions. We follow the same strategy to design the proposed human-like path planner for the robot navigation. Before introducing the planning method, we first explain how to modify the kinematic constraints in Sec.3.3 for calculation. Since the constraints in Eq.(1), and (2) are in the continuous form, they cannot be directly implemented in our proposed planning method. Thus we take the average velocity of robot into consideration for an easier implementation.

We assume that the robot would move from an arbitrary point ξ_i to an arbitrary goal ξ_j , with an initial heading angle θ . Then there exists the angular difference δ between θ and the vector representing the direction from ξ_i to ξ_j as

$$\delta(\theta, \xi_i, \xi_j) = \theta - \arctan \frac{y_j - y_i}{x_j - x_i} =: \delta_\theta \quad (3)$$

Therefore, in a complete motion for a robot from ξ_i with heading angle θ_i to ξ_j with θ_j , the robot can be regarded as under an average estimate of the constraint on translation (1) due to continuous change of heading angle. With abuse of $\xi = (x, y, \theta)$ to represent at point (x, y) with a robot heading angle of θ , we define the average constraint on translation as

$$F_{trans}(\xi_i, \xi_j) = \frac{\int_{\delta\theta_i}^{\delta\theta_j} f_{trans}(\delta\theta) d\theta}{\delta\theta_j - \delta\theta_i} \quad (4)$$

Similarly, an average estimate of the constraint on rotation (2) in the complete robot motion from ξ_i to ξ_j can be described as

$$F_{\text{rot}}(\theta_i, \theta_j) = \frac{1 - \gamma}{2} \cdot \cos\left(\frac{\theta_i + \theta_j}{2}\right) + \frac{1 + \gamma}{2} \quad (5)$$

By applying these two average estimates of constraints, Eq.(4) and Eq.(5), we can estimate the average speed v of the robot when moving from ξ_i to ξ_j in the proposed human-like manner.

$$v = v_{\max} \cdot F_{\text{trans}} \cdot F_{\text{rot}} \quad (6)$$

Based on the obstacle map, we apply the idea of heuristic search to compute the path from current robot position to the goal with minimum travelling time cost.

The optimization problem can be described with the following cost function

$$\min_{G_t} J = \sum_{k=0} G_t(\xi, \xi_0, v_{\text{des}})[k] + H_t(\xi, \xi_{\text{goal}}, v_{\text{est}})[k] \quad (7a)$$

$$\text{s.t. } v_{\text{des}} = v_{\max} \cdot F_{\text{trans}}(\xi, \xi_0) \cdot F_{\text{rot}}(\theta, \theta_0) \quad (7b)$$

$$v_{\text{est}} = v_{\max} \cdot F_{\text{trans}}(\xi_{\text{goal}}, \xi) \quad (7c)$$

where $G_t[k]$ denotes the time cost from the robot current pose $\xi_0(x_0, y_0, \theta_0)$ to the certain search point $\xi(x, y, \theta)$ at k^{th} search step. While the time cost $H_t[k]$ represents the estimated time from ξ to the goal $\xi_{\text{goal}}(x_{\text{goal}}, y_{\text{goal}}, \theta_{\text{goal}})$. ω_0 and ω denote the desired angular velocity of robot at ξ_0 and ξ , respectively. Similar as a classic A^* algorithm [16], the whole search process completes once $H_t[k] = 0$.

v_{des} is defined as the average translation speed from current position to the next search point, while v_{est} denotes an estimate of robot translation speed if the robot no longer changes its orientation from the next search point and keeps sliding movement to reach for the goal. The calculations follow the equations (4) and (5).

We solve the time-optimal problem by iterating the calculation of robot pose at each time step. At the k^{th} search step, a 3-dimensional search is executed. Namely, we first mesh the projected occupancy map in x, y plane with grids of 4×4 cm as one layer and divide the potential robot body orientation (360° in total) into 36 layers, 10° per layer. Any grid occupied with obstacle is regarded with a super high time cost. By assuming robot would turn its facing direction by a specific degree $\theta_i[k]$, $i = 1, \dots, 36$, we further calculate the time cost from current position to arbitrary search point at $(x_{\theta_i}, y_{\theta_i})$ one after another to obtain the minimum-costed in i^{th} layer. Finally, we compare all 36 $(x_{\theta_i}^{\min}, y_{\theta_i}^{\min})$ and take the exact search point $\xi_k(x_{\theta}^{\min}, y_{\theta}^{\min}, \theta[k])$ with the global minimum time cost for the robot. The desired pose ξ_k in each iteration is added into the path to generate. The $(k+1)^{\text{th}}$ search procedure repeats the calculation by replacing the current robot position with the x, y position of ξ_k .

4.4 Path Tracking

A simple path tracker is employed to command the robot to move to the desired pose $(x_{\text{des}}, y_{\text{des}}, \theta_{\text{des}})$ in the generated path. Counting from the goal, the calculated subgoal with shortest distance to the current robot position among all subgoals in the path is taken to follow. In case no subgoal is within a distance of 0.3m, the follower outputs infeasible and the path planner would subsequently

re-generate a path from current robot position to the goal. By inheriting the bounds of translational and rotational velocity from the path planning in Sec.4.3, the path tracker calculates a desired velocity (v_x, v_y, ω) and passes the output value at 10Hz.

4.5 Localization

Precise localization is needed in a complex environment, e.g. a typical store with many narrow corridors and moving customers. In our implementation, localization was achieved by combining the pointcloud data from the LiDAR and the bottom laser scanners, and the odometry inputs into a particle filter [13]. The particle filter tracked the pose of the robot at 10Hz.

4.6 Safety Limiter

A safety limiter module is additionally implemented before the velocity commands are executed by the robot. This module prevents the robot from approach dynamic obstacles by predicting the trajectories of the robot and dynamic obstacles in 1s at constant velocity. If any collision is predicted, the safety limiter would re-compute the maximum safe velocity in the same direction of the inherited velocity commands from path tracker.

4.7 Motion Planners for Benchmark

We also implemented other two modes of motion planner on the robot for comparison. A classic A^* path planner [16] was employed to generate paths from current robot position to the goal. Robot body orientation was not taken into account. Depending on different motion planning strategies, the desired body orientation at certain position was calculated as follows:

rotate-while-move: The robot rotation is separate from translation. The desired robot orientation is set as the goal orientation. The robot rotates at max angular velocity while moving.

rotate-then-move: The robot needs to stop translation when rotating. Thus we set the direction pointing to the closest position in the generated path as desired robot orientation. If this facing direction differs from current robot orientation, the robot would stop translation but rotate first.

5 EVALUATION FROM HUMAN TRAJECTORY

5.1 Method

To explore the impacts of the two constraints contributing to movement kinematics, we set up evaluations by comparing human trajectories with the robot trajectories generated by the proposed planner in the simulation of the same scenario. The real human trajectories were collected in a lab environment of $5\text{m} \times 2\text{m}$ covered by 6 Kinect cameras. A deep-learning based sensor networking system recognize moving people from depth image and real-time estimate their poses at 10Hz. Totally 80 participant trajectories in 5 different scenarios each with 4 different distance conditions were collected.

During the evaluation, we changed the parameters, namely α , β utilized in Eq.(1), and γ in Eq.(2), generated robot trajectories, and fitted them with human trajectories by accounting for the translation errors Δd and rotation errors $\Delta\theta$ between two, under the measurement of $D = \Delta\theta + \zeta\Delta d$. The parameters that generated trajectory with lowest error measure D were regarded as optimal.

In addition, since we expected to see how the constraint on translation and rotation matters respectively, we first calibrated the parameters under assumption that only one factor contributes to human movement. For instance, in the condition we ignored the impact of constraint on rotation, $f_{\text{rot}} = 1$, then the robot had not extra cost on changing body orientation. In contrast, if we ignored the influence of the constraint on moving direction, the robot would be able to move in any direction at full speed since $f_{\text{trans}} = 1$.

Therefore, the parameters were identified case by case in three condition, namely freezing $f_{\text{rot}} = 1$, freezing $f_{\text{trans}} = 1$, or taking both constraints into account. In each condition by fitting all trajectories, globally optimal parameters with lowest error measure were taken. We empirically decided $\zeta = 1$.

5.2 Results

Table 1 indicates the remaining error D after the calibration, with the optimum of parameters found through the calibration based on all 80 human trajectory data. The optimal combination of the parameters for the proposed method, which considered both kinematic constraints, led to the minimum remaining error $D = 9.92$. In contrast, $D = 10.21$ for the condition of $f_{\text{rot}} = 1$, and $D = 25.64$ for the condition of $f_{\text{trans}} = 1$. Our proposed method showed slightly better result than the condition of $f_{\text{rot}} = 1$. When compared with the condition of $f_{\text{trans}} = 1$, the error $\Delta\theta$ dropped. These indicated that considering both constraints could best resemble human movements, and the two constraints used in the proposed method both contribute. We also found that the major error fell on body orientation in with $f_{\text{trans}} = 1$. This indicates that the speed difference among specific movements (and its impact on body orientation) contributes more in human movements.

Table 1: Parameter calibration for kinematic constraints.

	α	β	γ	$\Delta\theta$	Δd	D
$f_{\text{rot}} = 1$	0.45	$\frac{7\pi}{9}$	-	8.02	2.19	10.21
$f_{\text{trans}} = 1$	-	-	0.05	22.47	2.17	25.64
proposed	0.3	$\frac{17\pi}{18}$	0.05	7.73	2.19	9.92

In Fig.7, we illustrate one of the human trajectories where the person turned 90° , moved forward 2m, and finally rotated back, as the blue trajectory in Fig.7a. Note that the arrows in the plots represent the pose of the human or robot at a constant time interval, with arrowhead denoting body orientation while the arrowroot showing the position. Fig.7b shows the trajectory in the condition of $f_{\text{rot}} = 1$, where robot rotated, slid to the goal and finally turned back. However, the heading angle during sliding quite differs from how human behaves. In the condition of $f_{\text{trans}} = 1$. The trajectory (see Fig.7c) is exactly in *rotate-while-move* strategy, as typical omnidirectional robot behavior. Fig.7d demonstrated that the proposed method generated a human-like motion, namely, first turned, then kept sliding and finally turned back before arriving at the goal.

6 USER STUDY

Due to the pandemic of covid-19, instead of an onsite user study, we conducted a video-based survey, in which participants were asked to watch a series of demonstration videos on robot navigation.

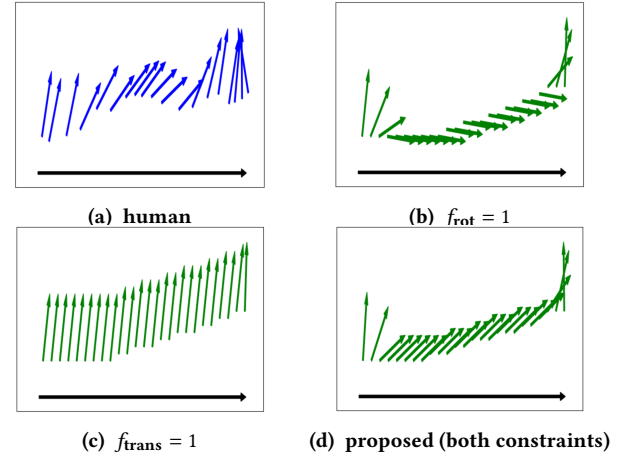


Figure 7: Human trajectory data versus simulated trajectories with different constraint configurations.

6.1 Hypothesis and Prediction

We designed the proposed method inspired from the observations of humans' natural movements. Therefore, we posited that a robot rotating its body with sliding in a human-inspired manner would be perceived more naturally (e.g. more human-like, elegantly) than a robot controlled in a purely functional way, like *rotate-then-move* or *rotate-while-move* strategies. In social interactions, these factors: natural, human-like, elegant can be grouped under the *anthropomorphism* label [1]. Thus, we made the following prediction:

- **Prediction 1 (“anthropomorphism”):** A robot using the proposed method gives participants the impression that it behaves more human-like compared to *rotate-then-move* and *rotate-while-move* strategies.

Meanwhile, human movement is with constraints, thus there exists speed difference among movements. Hence, we expected that a robot that reuses human kinematic constraints to reflect the speed difference can show its intents more explicitly and is more predictable than a robot with no speed difference. We group the factors like easy to understand, predictable under the label of *predictability*. We also expected a anthropomorphic and predictable robot to be preferred. Thus, we made the following predictions:

- **Prediction 2 (“predictability”):** A robot using the proposed method gives the impression that its motion is more predictable by participants than *rotate-then-move* and *rotate-while-move* strategies.
- **Prediction 3 (“likeability”):** Participants will prefer a robot using the proposed motion planning method than *rotate-then-move* and *rotate-while-move* strategies.

6.2 Method

6.2.1 Participants. We used external company to recruit 310 paid participants to take part in the study. After filtering out those participants who did not answer appropriately, e.g. scoring 1 or 7 for all of 1-to-7 point scales, we obtained results from the 300 participants ($N=300$; age: $M = 40$, $SD = 10.3$; 150 females).

6.2.2 Conditions. We compared the following three conditions:

- **rotate-then-move:** Typical differential-drive policy: A robot keeps its body orientation following the path direction, as described in Sec.4.7.
- **rotate-while-move:** Typical omni-directional policy: A robot simultaneously executes translation and rotation motions, as described in Sec.4.7.
- **proposed:** The proposed policy: A robot reaches for goals using the proposed planning approach in Sec.4.3.

The implementation of path planner (the green block in Fig.6) varied in each condition, while all other modules and robotic hardware were unchanged throughout the experiment.

6.2.3 Environment and Video stimuli. A robot navigation experiment was carried out in a sports souvenir store, which is with shelves full of products, low counters, and narrow corridors at width of 90 cm. It is a complex and challenging environment for a robot to execute safe navigation tasks.

The autonomous movements of the robot to achieve all the tasks were recorded as videos for participants to watch in the study. The robot was commanded to achieve navigation tasks inside the store, e.g. from a souvenir shelf to a clothing shelf, as daily occurred when a customer or a shop assistant looks for products in the shop. All tasks require the robot to change its body orientation appropriately when arriving. In each task, the robot autonomously moved collision-free at up to 0.9m/s. Each task took 10-20 seconds. The screenshots of robot navigation in three conditions are shown in Fig.8, 9 and 10. All videos are available in supplementary materials.

6.2.4 Procedure. The study had a within-participant design, and the order was counter-balanced. In each session, participants watched a video of robot navigating in 4 scenarios in one condition. The video includes text that informs in advance what robot would do (e.g. "the robot moves to the opposite side of the shelf") so that they can judge whether the robot's movements were predictable. After watching each video, they were asked to complete a questionnaire.

6.2.5 Measurement. The questionnaires (in Japanese) consisted of three component as follows, with 1-to-7 point Likert scales:

- **anthropomorphism** from [1], composed of 5 items: fake - natural, machine-like - human-like, unconscious - conscious, artificial - lifelike, moving rigidly - moving elegantly.
- **predictability** from [7], composed of 3 items (the movement of robot matched what I expected, the movement of robot is predictable, I would be surprised if the robot executed the movement in this situation.)
- **likeability** from [1], composed of 5 items (dislike - like, unfriendly - friendly, unkind - kind, unpleasant - pleasant, awful - nice).

6.3 Results

6.3.1 Anthropomorphism. First set of bars in Fig.11 presents the results from the anthropomorphism scale. Repeated-measures ANOVA revealed the significant effect of the conditions ($F(2, 598) = 9.216, p < .001, \eta_p^2 = .030$). Post-hoc analysis with Bonferroni method indicated the significant difference between the proposed method and *rotate-then-move* method ($p < .001$) and between the proposed method and *rotate-while-move* ($p = .024$). No significant difference was found between *rotate-then-move* and *rotate-while-move*.

($p = .373$). This result supports our prediction that: A robot using the proposed method gives participants a more anthropomorphic impression compared to other two strategies.

6.3.2 Predictability. Second set of bars in Fig.11 presents the results from the predictability scale. Repeated-measures ANOVA revealed the significant effect of the conditions ($F(2, 598) = 7.395, p = .001, \eta_p^2 = .024$). Post-hoc analysis with Bonferroni method indicated the significant difference between the proposed method and *rotate-while-move* ($p = .002$). No significant difference was found between the proposed method and *rotate-then-move* method ($p = .567$). There was significant difference between *rotate-then-move* and *rotate-while-move* ($p < .001$). The hypotheses of predictability was partially satisfied.

6.3.3 Likeability. Last set of bars in Fig.11 presents the results from the likeability scale. Repeated-measures ANOVA revealed the significant effect of the conditions ($F(2, 598) = 3.012, p = .049, \eta_p^2 = .011$). Post-hoc analysis with Bonferroni method identified only a statistical trend between the proposed method and *rotate-then-move* ($p = .0502$), and there was no significant difference between the proposed method and *rotate-while-move* method ($p = .489$) and between *rotate-then-move* and *rotate-while-move* ($p = .878$). The hypotheses of likeability was not satisfied.

7 DISCUSSION

7.1 Findings

The experimental results partially supported our hypotheses. We found that compared to other motion planning strategies, the proposed motion planner inspired from human movement left participants a more anthropomorphic impression. However, although the proposed method outperformed other strategies, many participants still rated it below 3, meaning that the robot behavior was still far from how human behaves.

Despite that the motion from our proposed planner was more anthropomorphic than other two methods and more predictable to participants compared to the *rotate-while-move* motion, there was no significant difference in preferences with the two methods. This might be because that participants linked their preferences to robots more to other factors like appearance instead of navigating motion, especially when watching videos.

7.2 Technical Implications

Since mobile robots with omni-directional bases are nowadays commercially available, it is possible to utilizing the proposed method into such robots. However, there exist concerns that need to be carefully addressed when implementing and testing this method. Due to the reason that the proposed method contains not only position information but also body orientation in the search, the method is more time-consuming for computation compared to many classic planning methods. For an arbitrary goal in a shop, it might take up to 1s to generate a path. Hence, a potential solution to use the proposed planning method in a large open space might be to first set up subgoals for robot navigation tasks.

Meanwhile, in our study, we found that body orientation of an omni-based robot in navigation contributes much to the intuitive feelings of human spectators. Therefore, for future designers who



Figure 8: Robot in rotate-then-move condition



Figure 9: Robot in rotate-while-move condition



Figure 10: Robot with proposed motion planner

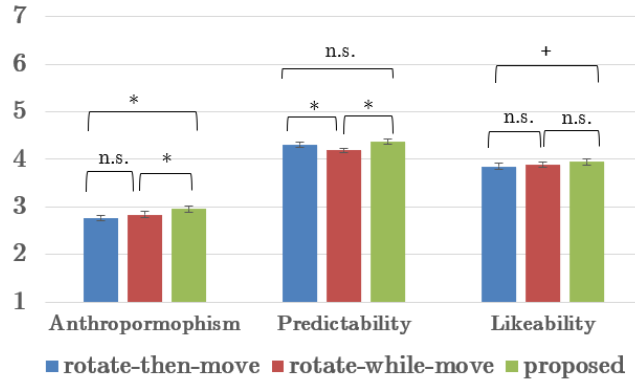


Figure 11: Results. Bars represents the SE. (N=300)

expect to deploy an omni-based robot for social applications, it is meaningful to pay more attention to robot body orientation.

7.3 Limitations

While showing the importance of body orientation and speed difference in various directions for robot motion planning, this work still possesses limitations. First, we conducted this research in Japan, thus whether similar results translate in other regions of the world might be difficult to confirm. However, since the parameters in the proposed method are calibrated through human trajectory data, it

would be possible to apply the proposed method in other countries after recalibration of parameters. In addition, we used robot navigation videos in our experiment. Compared to the onsite demonstrations, video experiments may to some extent affect the research results as participants have less feelings of presence than they standing nearby and watching robot moving. Finally, this research was carried out with a specific humanoid robot. However, mobile robots with omni-base are not limited with faces, thus future work could be done with a non humanoid robot, e.g. a robotic vehicle.

8 CONCLUSION

In this paper, we explored how humans naturally move. Based on the observations, we proposed that human movement suffices to a global time-efficient optimization strategy under certain kinematic constraints, and developed a time optimal motion planner inspired from the human movements for omni-directional robots to behave in a more natural manner in navigation. Results of 300 participants showed that our proposed method provided the human spectators with feelings that the robot behaves more human-like and predictable compared to other motion planning strategies.

ACKNOWLEDGMENTS

This research was in part supported by JST CREST Grant Number JPMJCR17A2, Japan, and in part supported by JSPS KAKENHI Grant Number JP18H04121. The authors would like to thank Hiromi Kobayashi for her help on the user study.

REFERENCES

- [1] Christoph Bartneck, Elizabeth Croft, and Dana Kulic. 2009. Measurement instruments for the anthropomorphism, animacy, likeability, perceived intelligence, and perceived safety of robots. *International Journal of Social Robotics* 1, 1 (2009), 71–81. <https://doi.org/10.1007/s12369-008-0001-3>
- [2] Wolfram Burgard, Armin B. Cremers, Dieter Fox, Dirk Hähnel, Gerhard Lakemeyer, Dirk Schulz, Walter Steiner, and Sebastian Thrun. 1999. Experiences with an interactive museum tour-guide robot. *Artificial Intelligence* 114, 1 (1999), 3–55.
- [3] S. Chamberland, É. Beaudry, L. Clavien, F. Kabanza, F. Michaud, and M. Lauriat. 2010. Motion planning for an omnidirectional robot with steering constraints. In *Proceedings of the 2010 IEEE/RSJ International Conference on Intelligent Robots and Systems*. 4305–4310.
- [4] Y. Che, A. M. Okamura, and D. Sadigh. 2020. Efficient and Trustworthy Social Navigation via Explicit and Implicit Robot–Human Communication. *IEEE Transactions on Robotics* 36, 3 (2020), 692–707.
- [5] Y. F. Chen, M. Everett, M. Liu, and J. P. How. 2017. Socially aware motion planning with deep reinforcement learning. In *Proceedings of the 2017 IEEE/RSJ International Conference on Intelligent Robots and Systems (IROS)*. 1343–1350.
- [6] S. Devin and R. Alami. 2016. An implemented theory of mind to improve human–robot shared plans execution. In *2016 11th ACM/IEEE International Conference on Human-Robot Interaction (HRI)*. 319–326.
- [7] Anca Dragan and Siddhartha Srinivasa. 2014. Familiarization to Robot Motion. In *Proceedings of the 2014 ACM/IEEE International Conference on Human-Robot Interaction (HRI '14)*. Association for Computing Machinery, New York, NY, USA, 366–373. <https://doi.org/10.1145/2559636.2559674>
- [8] A. D. Dragan, S. Bauman, J. Forlizzi, and S. S. Srinivasa. 2015. Effects of Robot Motion on Human–Robot Collaboration. In *2015 10th ACM/IEEE International Conference on Human-Robot Interaction (HRI)*. 51–58.
- [9] A. D. Dragan, K. C. T. Lee, and S. S. Srinivasa. 2013. Legibility and predictability of robot motion. In *2013 8th ACM/IEEE International Conference on Human-Robot Interaction (HRI)*. 301–308.
- [10] G. Ferrer and A. Sanfeliu. 2014. Behavior estimation for a complete framework for human motion prediction in crowded environments. In *Proceedings of the 2014 IEEE International Conference on Robotics and Automation (ICRA)*. 5940–5945.
- [11] D. Fox, W. Burgard, and S. Thrun. 1997. The dynamic window approach to collision avoidance. *IEEE Robotics and Automation Magazine* 4, 1 (1997), 23–33.
- [12] M. A. Goodrich and D. R. Olsen. 2003. Seven principles of efficient human–robot interaction. In *Proceedings. 2003 IEEE International Conference on Systems, Man and Cybernetics*, Vol. 4. 3942–3948.
- [13] G. Grisetti, C. Stachniss, and W. Burgard. 2007. Improved Techniques for Grid Mapping With Rao–Blackwellized Particle Filters. *IEEE Transactions on Robotics* 23, 1 (2007), 34–46.
- [14] Keenon Robotics Group. 2019. Peanut: Autonomous Commercial Service Robot. <http://www.keenon.com/EN/Product/pro1.html>
- [15] SoftBank Robotics Group. 2019. Pepper the humanoid and programmable robot: SoftBank Robotics. <https://www.softbankrobotics.com/emea/en/pepper>
- [16] P. E. Hart, N. J. Nilsson, and B. Raphael. 1968. A Formal Basis for the Heuristic Determination of Minimum Cost Paths. *IEEE Transactions on Systems Science and Cybernetics* 4, 2 (1968), 100–107.
- [17] Sujeong Kim, Stephen J. Guy, Wenxi Liu, David Wilkie, Rynson W.H. Lau, Ming C. Lin, and Dinesh Manocha. 2015. BRVO: Predicting pedestrian trajectories using velocity-space reasoning. *The International Journal of Robotics Research* 34, 2 (2015), 201–217.
- [18] Henrik Kretzschmar, Markus Spies, Christoph Sprunk, and Wolfram Burgard. 2016. Socially compliant mobile robot navigation via inverse reinforcement learning. *The International Journal of Robotics Research* 35, 11 (2016), 1289–1307.
- [19] Thibault Kruse, Amit Kumar Pandey, Rachid Alami, and Alexandra Kirsch. 2013. Human-Aware Robot Navigation: A Survey. *Robotics and Autonomous Systems* 61 (12 2013), 1726–1743.
- [20] Xiang Li and Andreas Zell. 2007. Motion Control of an Omnidirectional Mobile Robot. In *Proceedings of the 2007 International Conference on Informatics in Control, Automation and Robotics*, Vol. 24. 125–132.
- [21] M. Luber, L. Spinello, J. Silva, and K. O. Arras. 2012. Socially-aware robot navigation: A learning approach. In *Proceedings of the 2012 IEEE/RSJ International Conference on Intelligent Robots and Systems*. 902–907.
- [22] K. Mizumaru, S. Satake, T. Kanda, and T. Ono. 2019. Stop Doing it! Approaching Strategy for a Robot to Admonish Pedestrians. In *2019 14th ACM/IEEE International Conference on Human-Robot Interaction (HRI)*. 449–457.
- [23] M. Phillips and M. Likhachev. 2011. SIPP: Safe interval path planning for dynamic environments. In *Proceedings of the 2011 IEEE International Conference on Robotics and Automation*. 5628–5635.
- [24] Jorge Rios-Martinez, Anne Spalanzani, and Christian Laugier. 2014. From Proxemics Theory to Socially-Aware Navigation: A Survey. *International Journal of Social Robotics* 7 (04 2014), 137–153.
- [25] Emmanuel Senft, Satoru Satake, and Takayuki Kanda. 2020. Would You Mind Me If I Pass by You? Socially-Appropriate Behaviour for an Omni-Based Social Robot in Narrow Environment. In *Proceedings of the 2020 ACM/IEEE International Conference on Human-Robot Interaction*. 539–547.
- [26] Masahiro Shiomi, Francesco Zanlungo, Kotaro Hayashi, and Takayuki Kanda. 2014. Towards a Socially Acceptable Collision Avoidance for a Mobile Robot Navigating Among Pedestrians Using a Pedestrian Model. *International Journal of Social Robotics* 6, 3 (2014), 443–455.
- [27] Annemarie Turnwald and D. Wollherr. 2019. Human-Like Motion Planning Based on Game Theoretic Decision Making. *International Journal of Social Robotics* 11 (2019), 151–170.
- [28] F. Zanlungo, T. Ikeda, and T. Kanda. 2011. Social force model with explicit collision prediction. *EPL (Europhysics Letters)* 93, 6 (mar 2011), 68005.
- [29] Y. Zhang, S. Sreedharan, A. Kulkarni, T. Chakraborti, H. H. Zhuo, and S. Kambhampati. 2017. Plan explicability and predictability for robot task planning. In *2017 IEEE International Conference on Robotics and Automation (ICRA)*. 1313–1320.